ConF-900641--1

LBL-28517

Center for Advanced Materials

CAM

Presented at the International Conference on Advanced Aluminum and Magnesium Alloys, Amsterdam, June 20–22, 1990, and to be published in the Proceedings

Fatigue-Crack Propagation in Aluminum-Lithium Alloys Processed by Powder and Ingot Metallurgy

K.T. Venkateswara Rao, N.J. Kim, P.P. Pizzo, and R.O. Ritchie

April 1990

Materials and Chemical Sciences Division

Lawrence Berkeley Laboratory • University of California

ONE CYCLOTRON ROAD, BERKELEY, CA 94720 • (415) 486-4755

Prepared for the U.S. Department of Energy under Contract DE-AC03-76SF00098

LBL--28517

DE92 000904

FATIGUE-CRACK PROPAGATION IN ALUMINUM-LITHIUM ALLOYS PROCESSED BY POWDER AND INGOT METALLURGY

K. T. Venkateswara Rao,[1] N. J. Kim,[2] P. P. Pizzo[3] and R. O. Ritchie[1]

[1]Center for Advanced Materials, Lawrence Berkeley Laboratory
and
Department of Materials Science and Mineral Engineering
University of California, Berkeley, CA 94720

[2]Pohang Institute of Science and Technology, Pohang, 790-330, Korea

[3]San Jose State University, San Jose, CA 95192

April 1990

to be presented at the *International Conference on Advanced Aluminum and Magnesium Alloys*, Amsterdam, June 1990, ASM European Office, 1990

This work was supported by the Director, Office of Energy Research, Office of Basic Energy Sciences, Materials Sciences Division, of the U.S. Department of Energy under Contract No. DE-AC03-76SF00098.

FATIGUE-CRACK PROPAGATION IN ALUMINUM-LITHIUM ALLOYS PROCESSED BY POWDER AND INGOT METALLURGY

K. T. Venkateswara Rao[1], N. J. Kim[2], P. P. Pizzo[3], and R. O. Ritchie[1]

[1]University of California, Berkeley, CA 94720, USA
[2]Pohang Institute of Science and Technology, Pohang, 790-330 Korea*
[3]San José State University, San Jose, CA 95192, USA

ABSTRACT

Fatigue-crack propagation behavior in powder-metallurgy (P/M) aluminum-lithium alloys, namely, mechanically-alloyed (MA) Al-4.0Mg-1.5Li-1.1C-0.8O_2 (Inco 905-XL) and rapid-solidification-processed (RSP) Al-2.6Li-1.0Cu-0.5Mg-0.5Zr (Allied 644-B) extrusions, has been studied, and results compared with data on an equivalent ingot-metallurgy (I/M) Al-Li alloy, 2090-T81 plate. Fatigue-crack growth resistance of the RSP Al-Li alloy is found to be comparable to the I/M Al-Li alloy; in contrast, crack velocities in MA 905-XL extrusions are nearly three orders of magnitude faster. Growth-rate response in both P/M Al-Li alloys, however, is highly anisotropic. Results are interpreted in terms of the microstructural influence of strengthening mechanism, slip mode, grain morphology and texture on the development of crack-tip shielding from crack-path deflection and crack closure.

INTRODUCTION

Considerable research work over the past few years (1-7), has focussed on the development of ultra-low density aluminum-lithium alloys using powder-metallurgy (P/M) processing methods. The principal objective of these efforts has been to improve the ductility and fracture properties of Al-Li alloys, particularly when fabricated as extrusions and forgings, because complex thermomechanical treatments often employed on ingot-metallurgy (I/M) plate and sheet products are not feasible. Two techniques of P/M processing, namely, rapid-solidification processing (RSP) and mechanical alloying (MA), have attracted the most attention and have been commercially successful in the development of Al-Li alloy extrusions (2-5). With RSP, the powders are prepared by pulverizing melt-spun ribbons, that are solidified at cooling rates exceeding 10^6 °C/sec (2). Mechanical alloying, on the other hand, involves dry,

---

*Formerly at Metals and Ceramics Lab., Allied-Signal Inc., Morristown, NJ 07960, USA.

high-energy milling to produce composite powders by continuously fracturing and rewelding various metallic and non-metallic elemental powders (4-6). The powders are then consolidated by vacuum hot pressing and finally extruded or forged to the required product form.

The objective of the present study is to examine the fatigue-crack growth behavior in two of the more prominent P/M Al-Li alloys, mechanically-alloyed IncoMAP AL 905-XL, containing Mg, C and O_2 additions, and rapidly-solidified Allied-Signal 644-B, containing Cu, Mg and Zr additions (2,6), and to compare results with an I/M Al-Li alloy 2090-T81 plate (8). This is deemed to be important as many wrought I/M Al-Li alloys are known to exhibit superior fatigue-crack propagation resistance to most traditional high-strength aluminum alloys, due to enhanced crack-tip shielding from crack deflection and crack closure promoted by crystallographic crack advance in coarse, unrecrystallized and textured planar-slip microstructures (8,9). However, it is uncertain whether such effects will be seen in the more isotropic, fine-grained P/M microstructures.

EXPERIMENTAL PROCEDURES

P/M mechanically-alloyed IncoMAP-AL 905-XL (Al-Li-Mg-C-O) and RSP Allied-Signal 644-B (Al-Li-Cu-Mg-Zr) alloys were received as rectangular extrusions with cross-sections 50 x 12 and 100 x 25 mm^2, respectively. Chemical compositions and grain-size dimensions are compared to I/M Al-Li-Cu-Zr alloy 2090-T81 in Table 1.

Table 1 Chemical compositions and grain size of alloys tested

Alloy	Composition (wt.%)							Grain Size* (μm)		
	Li	Cu	Mg	Zr	C	O	Al	L	T	S
MA AL 905-XL	1.5	-	4.0	-	1.1	0.8	bal	1-2	0.4	0.3
RSP 644-B	2.6	1.0	0.5	0.5	-	-	bal	5-10	1-2	1-2
I/M 2090	2.1	2.9	-	0.1	-	-	bal	2000	500	50

*L, T and S refer to longitudinal, long-transverse and short-transverse directions

Microstructures in MA P/M AL 905-XL extrusions, which were peak aged at 170°C for 24 h, were relatively equiaxed with extremely fine grains (Fig. 1), stabilized by dispersions of 20-50 nm sized Al_2O_3 and Al_4C particles formed during ball milling (4-6). Some grains and dispersoids were elongated ~1-2 μm in the extrusion direction (E/D); dimensions normal to the E/D are typically 0.3-0.5 μm. In other words, grain morphologies were rod-like and resembled ultrafine aligned-fiber composites. Strengthening is achieved primarily by dispersion hardening from oxides and carbides, and dislocation substructures retained during powder processing; both Li and Mg remain in solid solution, thereby suppressing the formation of metastable δ' (Al_3Li) or equilibrium Al_2LiMg precipitates (4-6). Structures in the RSP 644-B extrusions, underaged at 135°C for 16 h, consisted primarily of composite-δ' coating β' (Al_3Zr) dispersoids and monolithic δ' spheres; S (Al_2CuMg) laths, T_1 (Al_2CuLi) plates and heterogenous grain-boundary precipitation were completely absent (Fig. 2). Corresponding RSP grain structures were far finer than in I/M alloys (Fig. 1), but coarse compared to the MA material; grains were unrecrystallized and stretched along the E/D (typically 5-10 μm in length and 1-2 μm in diameter). Mechanical properties of these P/M extrusions are compared to wrought I/M 2090-T81 plates in Table 2.

Table 2 Room temperature mechanical properties of P/M and I/M Al-Li alloys tested†

Alloy	Yield Strength (σ_y (MPa)	Tensile Strength (MPa)	Percent Elongation (on 25 mm)	Fracture Toughness K_{Ic} (MPa√m)	Strain Hardening Exponent n
AL 905-XL	559	596	2.3	13 (L-T) 13 (S-L)	--
644-B	422	539	7.7	24 (L-T) 10 (S-L)	0.19
2090-T81	552	589	11.0	36 (L-T) 17 (S-L)	0.06

†Tensile properties in the longitudinal (L) direction

Fatigue-crack growth tests were conducted on through-thickness long (>5 mm) cracks, using 10-mm-thick compact tension specimens (L-T, T-L orientations), in controlled room-temperature air (22°C, 45% relative humidity) at load ratios ($R = K_{min}/K_{max}$) of 0.10 and 0.75 (50 Hz sinsuoidal frequency). Tests were performed under stress-intensity control on automated servohydraulic testing machines, using d.c. electrical-potential and back-face strain elastic-compliance methods to monitor crack length and crack closure, respectively (10). Growth-rate (da/dN) results on P/M alloys are presented, both in terms of the nominal ($\Delta K = K_{max}-K_{min}$) and effective ($\Delta K_{eff} = K_{max}-K_{cl}$) stress-intensity ranges, and compared with those in I/M 2090-T81 Al-Li alloy plate; the latter material shows the best fatigue-crack propagation resistance of commercial I/M Al-Li alloys (8,11).

RESULTS

Fatigue-crack propagation behavior in P/M Al-Li alloys, MA AL 905-XL and RSP 644-B (L-T orientation), at R = 0.1, is compared in Fig. 3a with results on I/M alloy 2090-T81 (8,11); corresponding crack-closure data are plotted in Fig. 3b. The sub-micron grained MA 905-XL extrusions are seen to exhibit the fastest crack-growth rates, roughly 2 to 3 orders of magnitude higher than coarse-grained I/M alloy 2090-T81 at equivalent ΔK levels, for all growth-rates ranging between the fatigue threshold (ΔK_{TH}) and instability (K_{Ic}); the ΔK_{TH} value is also ~36% lower compared to 2090. The coarser-grained RSP 644-B alloy shows far superior crack-growth resistance; growth rates are comparable to 2090-T81, with a ~10% higher fatigue threshold.

Qualitatively, such behavior is consistent with measured variations in crack closure (Fig. 3b); values for K_{cl} in the RSP P/M alloy are comparable to those in I/M 2090-T81 and approach 80% of K_{max}, close to ΔK_{TH}. Conversely, in the mechanically-alloyed P/M material, closure levels remain low and only approach 40% of K_{max} at ΔK_{TH}. These differences in closure can in turn be traced to the morphological variations in fatigue-crack paths and resulting fracture surfaces (Fig. 4). For example, the faster crack velocities and low closure levels seen in MA 905-XL microstructures are associated with markedly linear crack paths (Fig. 4c) and relatively smooth, transgranular fatigue surfaces (Fig. 4f), showing little evidence for crystallographic cracking. Fractographic features in the RSP 644-B alloy (Figs. 4b,e), on the other hand, resemble those seen in I/M Al-Li alloys, which deform by planar slip; crack paths are highly deflected and fracture surfaces display evidence of local slip-band cracking similar to 2090 (Figs. 4a,d). In addition, differences in crack-path tortuousity, as observed across the specimen thickness perpendicular to the crack plane, are also apparent (Fig. 5). In MA 905-XL extrusions, the crack front is planar due to the lack of deformation texture in the material; by contrast, the RSP 644-B alloy shows a more faceted and crystallographic profile. This is to be compared with the highly-textured I/M 2090-T81 alloy, where the crack front exhibits unusually sharp facets with an included angle of ~60°, resulting from crack advance along intersecting (111) planes (12). Such faceted fracture morphologies, coupled with small crack-tip shear displacements, can promote premature wedging of fracture-surface asperities during fatigue, both along the crack front and in the direction of crack growth, thus promoting three-dimensional roughness-induced crack closure.

Similar to behavior in I/M Al-Li plates (8), crack-growth rates in both P/M alloys are dependent upon specimen orientation; crack velocities are over two orders of magnitude faster in the T-L orientation than in the L-T, especially at near-threshold ΔK levels (Fig. 6). As crack advance in the T-L orientation is parallel to the extrusion direction E/D (along the aligned rod-like grains) with a linear crack profile, closure levels are lower and growth rates are faster compared to L-T, where cracking proceeds perpendicular to the E/D.

Growth rates in both P/M Al-Li alloys are also sensitive to load ratio (Fig. 7), typical of most metallic materials (13); with increasing R, crack-growth rates are increased and ΔK_{TH} values correspondingly reduced as the effect of closure from crack-wedging gradually diminishes. The influence of R is particularly marked in the RSP 644-B alloy owing to the high levels of closure developed at $R = 0.1$, but is less pronounced in the 905-XL alloy since overall crack-closure levels are much lower.

DISCUSSION

The present results illustrate the marked differences in (long) fatigue-crack propagation behavior of P/M Al-Li alloys processed by various techniques. At low (positive) load ratios, rapidly-solidified 644-B extrusions display consistently slower growth rates for all ΔK levels compared to the mechanically-alloyed material; behavior is in fact quite similar to I/M 2090-T81 plate. Such trends are consistent with the degree to which crack-tip shielding is promoted microstructurally in these alloys. Growth rates are the fastest in MA 905-XL microstructures, which exhibit extremely linear crack paths and consequently the lowest (roughness-induced) closure levels; conversely, RSP 644-B and I/M 2090-T81 alloys develop far greater closure levels, by virtue of their highly deflected crack morphologies, and correspondingly show much slower crack-propagation rates.

The effect of deflected crack paths is to retard crack advance by increasing the path length traversed by the crack, reducing the *local* "crack-driving force" by deviating the crack off the plane of maximum tensile stress, and most importantly inducing high closure levels from wedging of fracture-surface asperities (11). Microstructurally, such morphological variations in fatigue-crack path result from differences in slip character or hardening mechanism, grain size, aging temper and deformation texture (11,12). In RSP 644-B alloy, the deflected crack profiles are due to inhomogenous planar-slip deformation, concentrated within narrow {111} slip bands, resulting in crystallographically-faceted crack extension (slip-band cracking) along intersecting sets of {111} planes (Figs. 4b,e). This results from the presence of coherent, ordered δ' precipitates that are readily sheared by moving dislocations, and by the β' dispersoids, which impart preferred orientations to grains by inhibiting recrystallization (following warm working), thereby restricting deformation to fewer, more favorably-oriented slip systems. As planar slip is prevalent in the P/M 644-B alloy despite its fine grain size, crack-closure levels and consequently crack-growth rates remain comparable to I/M Al-Li alloys, which similarly derive high closure levels from coherent δ'-induced and texture-induced deflected crack paths.

In contrast, such marked effects of slip planarity and texture on crack closure and crack-growth rates are essentially non-existent in mechanically-alloyed 905-XL extrusions, where deformation is more homogeneous due to strengthening primarily from oxide and carbide dispersions. Consequently, crack propagation in this alloy shows no evidence for slip-band cracking; fatigue-crack paths are thus highly linear (Figs. 4c,f), closure levels are far lower, and crack velocities are correspondingly much faster (Fig. 3).

With the exception of MA material, fatigue-crack growth rates in most Al-Li alloys are strongly dependent on the crack-path morphology and resulting crack closure; behavior is thus very sensitive to specimen orientation, specifically in terms of the crack-path direction in relation to microstructure and grain orientation. In I/M rolled plate, where grains tend to be laminated (Fig. 1c), poor crack-growth resistance is found where cracks run parallel to the laminated grains, i.e., S-T and S-L orientations (8). The grain structures in P/M extrusions, conversely, resemble aligned-fiber composites (Figs. 1a,b); the lowest resistance to crack growth is now found where cracks are oriented parallel to the "fibers", i.e., T-L and S-L orientations. However, since the sources of closure from planar slip, grain morphology and texture are minimized in mechanically-alloyed P/M alloys, crack-growth resistance in MA 905-XL is more isotropic (Fig. 6).

Additionally, the dependency of crack-growth rate behavior on the load ratio is a strong function of crack closure. Similar to results in other high-strength P/M aluminum alloys (14), this phenomenon is particularly marked in the RSP alloy. K_{cl} values approach 75% of K_{max}, close to ΔK_{TH}; load ratios above 0.75 are thus required to suppress the effect of closure from crack-wedging mechanisms. In the MA material, conversely, K_{cl} values remain below 40% of K_{max}; the sensitivity to load ratio is therefore maximized below $R = 0.4$ such that differences between growth rates at $R = 0.1$ and 0.75 are far less apparent (Fig. 7). However, when crack-growth data are compared at high load ratios ($R = 0.75$) as in Fig. 7, or plotted in terms of the closure-corrected ΔK_{eff} parameter (11), behavior in the two P/M alloys is more or less identical and similar to many I/M Al-Li alloys, implying that most differences in fatigue-crack propagation resistance of Al-Li alloys with respect to microstructure, orientation and load ratio stem principally from variations in crack closure.

CONCLUSIONS

Based on a study of fatigue-crack propagation in P/M Al-Li alloys processed through rapid solidification (Allied 644-B) and mechanical alloying (Inco 905-XL), the following conclusions can be made:

1. Fatigue-crack propagation rates in mechanically-alloyed P/M Al-Li alloy 905-XL, at R = 0.1, are approximately three orders of magnitude faster than in I/M Al-Li alloy 2090-T81 at equivalent ΔK levels. Conversely, crack velocities in rapidly-solidified P/M 644-B alloy are comparable to 2090-T81.

2. Such marked differences in crack-growth behavior between the two P/M Al-Li alloys are associated with microstructurally-induced variations in crack-tip shielding. In RSP 644-B alloy, crack paths are highly deflected, which promote high (roughness-induced) crack-closure levels, similar to I/M Al-Li alloys. In contrast, profiles in the MA 905-XL are unusually linear; measured closure levels are therefore lower, resulting in a comparatively higher ΔK_{eff} at the crack-tip and hence faster crack-growth rates.

3. Akin to I/M Al-Li plate alloys, the tortuosity of crack paths in RSP 644-B alloy is associated with crystallographic crack advance induced by planarity of slip due to coherent δ'-precipitation hardening and pronounced texture. Such beneficial effects of Li on fatigue resistance are not evident in the more isotropic MA Al-Li-Mg extrusions, which conversely derive their strength from oxide- and carbide-dispersion hardening.

4. Growth-rate behavior in P/M 644-B extrusions is highly anisotropic. Due to the aligned, needle-shaped and unrecrystallized grain structures in extruded sections, growth rates in the T-L orientation are up to 2-3 orders of magnitude faster than in the L-T. Such differences are less apparent in the more isotropic MA 905-XL material.

5. Due to the higher crack-closure levels, load-ratio effects are more pronounced in the RSP alloy than in the MA material. However, when crack-growth data are compared at high R, where closure effects are suppressed, differences in fatigue-crack growth resistance between the two P/M Al-Li extrusions are less apparent; in fact behavior becomes comparable to I/M Al-Li plate alloys.

ACKNOWLEDGEMENTS

This work was supported by the Director, Office of Energy Research, Office of Basic Energy Sciences, Materials Sciences Division, of the U.S. Department of Energy under Contract No. DE-AC03-76SF00098. Thanks are due to Drs. W. E. Quist (Boeing) and H. G. Nelson (NASA-Ames Research Center) for providing the P/M alloys, and to J. C. McNulty for experimental assistance.

REFERENCES

(1) W. E. Quist, G. H. Narayanan, A. L. Wingert and T. M. F. Ronald, in *Aluminium-Lithium Alloys III*, C. Baker, P. J. Gregson, S. J. Harris and C. J. Peel, eds., Institute of Metals, London, U.K. (1986), 625.

(2) N. J. Kim, R. L. Bye and S. K. Das, *J. Physique Coll.*, C3:9 (1987), 309.

(3) P. J. Meschter, J. K. Gregory, R. J. Lederich, J. E. O'Neal, E. J. Lavernia and N. J. Grant, *ibid.*, 317.

(4) P. S. Gilman, in *Aluminum-Lithium Alloys II*, T. H. Sanders and E. A. Starke, eds., TMS-AIME, Warrendale, PA (1983), 485.

(5) S. J. Donachie and P. S. Gilman, *ibid.*, 507.

(6) R. D. Schelleng, *J. Metals*, 41:1 (1989), 32.

(7) R. S. Sundaresan and F. H. Froes, *J. Metals*, 39:8 (1987), 15.

(8) K. T. Venkateswara Rao, W. Yu and R. O. Ritchie, *Metall. Trans. A*, 19A (1988), 549.

(9) A. K. Vasudévan, R. D. Doherty and S. Suresh, *Treatise on Mater. Sci. Technol.*, 31 (1989), 445.

(10) R. O. Ritchie and W. Yu, in *Small Fatigue Cracks*, R. O. Ritchie and J. Lankford, eds., TMS-AIME, Warrendale, PA (1986), 167.

(11) K. T. Venkateswara Rao and R. O. Ritchie, *Mater. Sci. Technol.*, 5 (1989), 896.

(12) G. R. Yoder, P. S. Pao, M. A. Imam and L. A. Cooley, *Scripta Metall.*, 22 (1988), 1241.

(13) S. Suresh and R. O. Ritchie, *Eng. Fract. Mech.*, 18 (1983), 785.

(14) K. Minakawa, G. Levan and A. J. McEvily, *Metall. Trans. A*, 17A (1986), 1787.

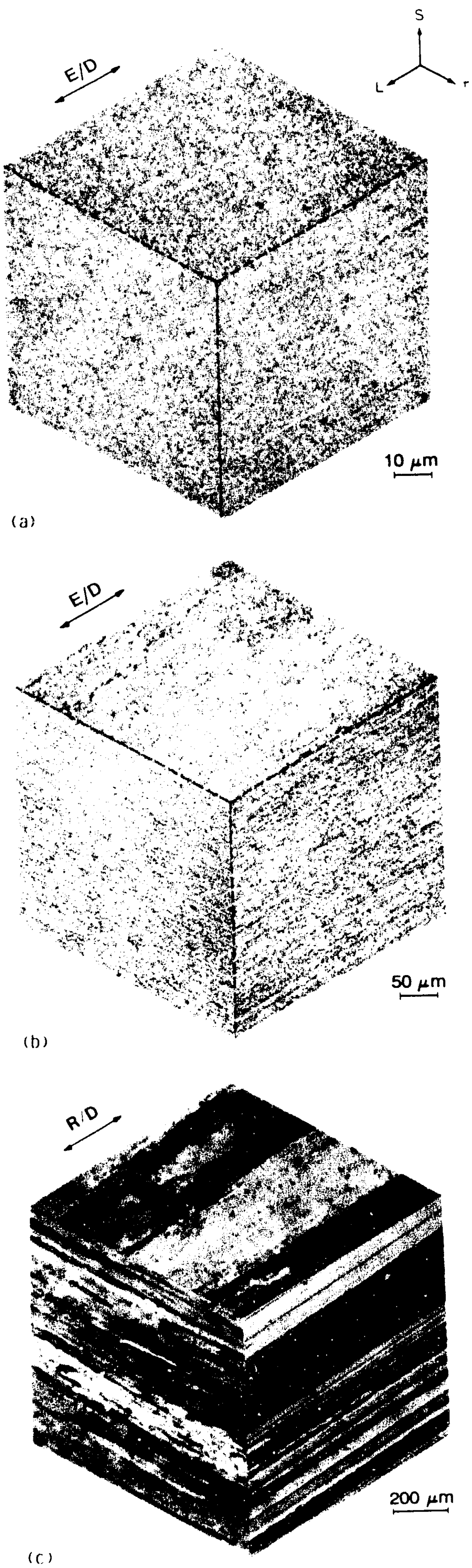

FIG. 1

Optical micrographs of grain structures in P/M Al-Li alloy extrusions processed by (a) mechanical alloying (AL 905-XL) and (b) rapid solidification (RSP 644-B), compared to (c) I/M 2090-T81 Al-Li alloy plate. (XBB 864-3075E)

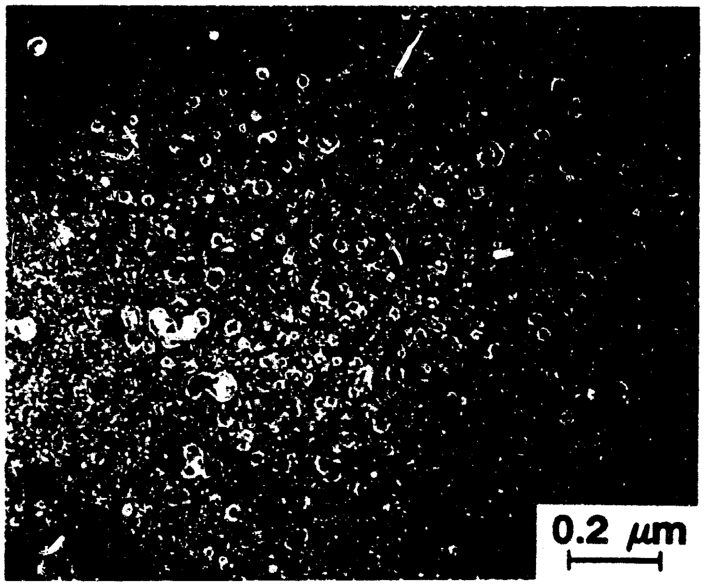

FIG. 2

Transmission electron micrograph illustrating the predominant microstructural features and hardening precipitates in RSP 644-B P/M Al-Li alloy (aged 16 h at 135°C, showing ordered δ' (Al_3Li) spheres and composite δ' particles surrounding β' (Al_3Zr) dispersoids. Imaging done under dark-field conditions using δ' (100) super-lattice reflections. (XBB 902-1131)

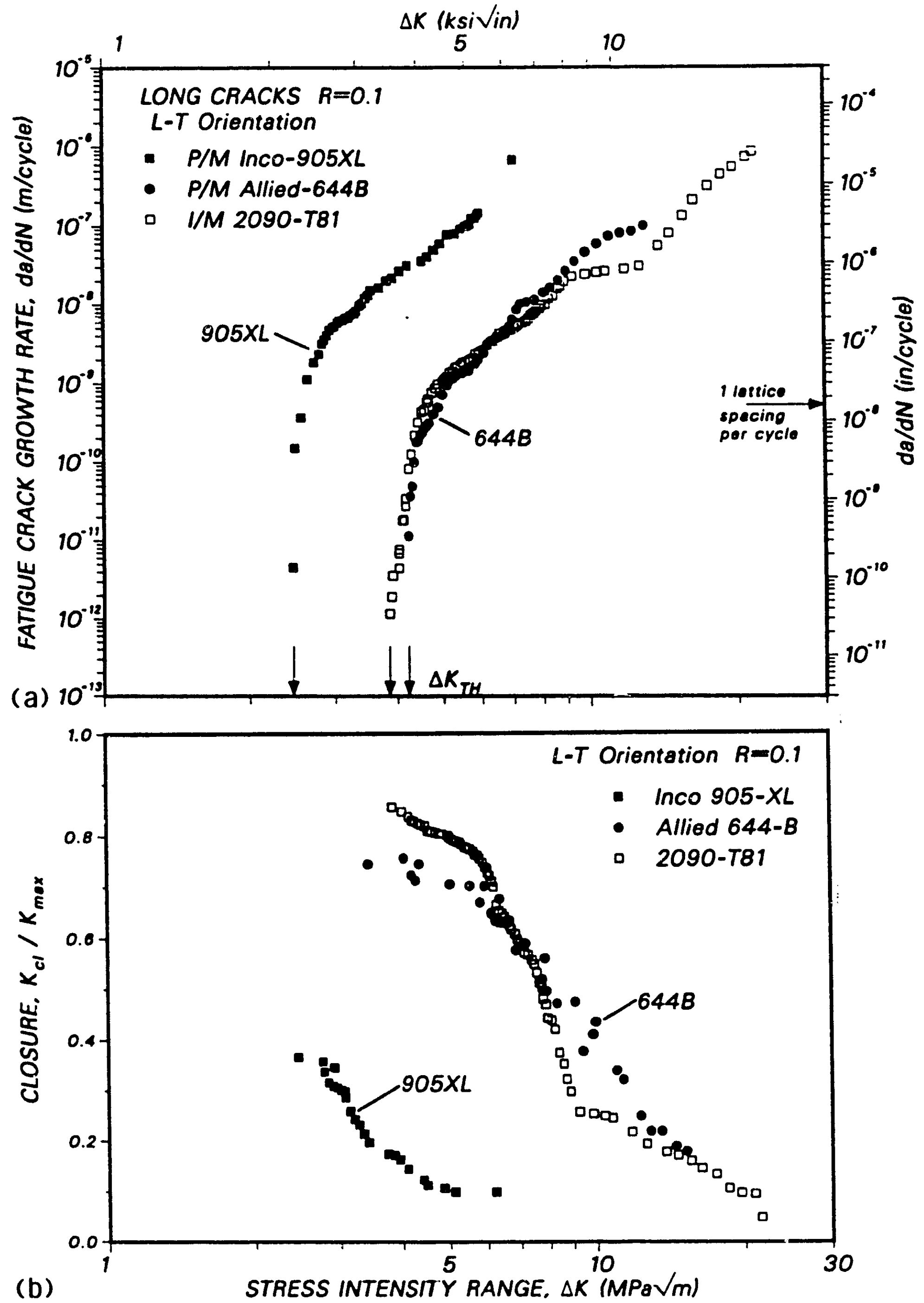

XBL 901-256

FIG. 3

(a) Fatigue-crack growth and (b) crack-closure behavior in MA AL 905-XL and BSP 644-B P/M Al-Li alloys, compared with peak-aged I/M 2090-T81 (R = 0.1, L-T orientation). Note that growth rates in 905-XL extrusions are significantly faster, consistent with much lower crack-closure levels. Data on 2090-T81 taken from Ref. 8. The closure stress intensity, K_{cl}, is defined at first contact of the fracture surfaces on unloading.

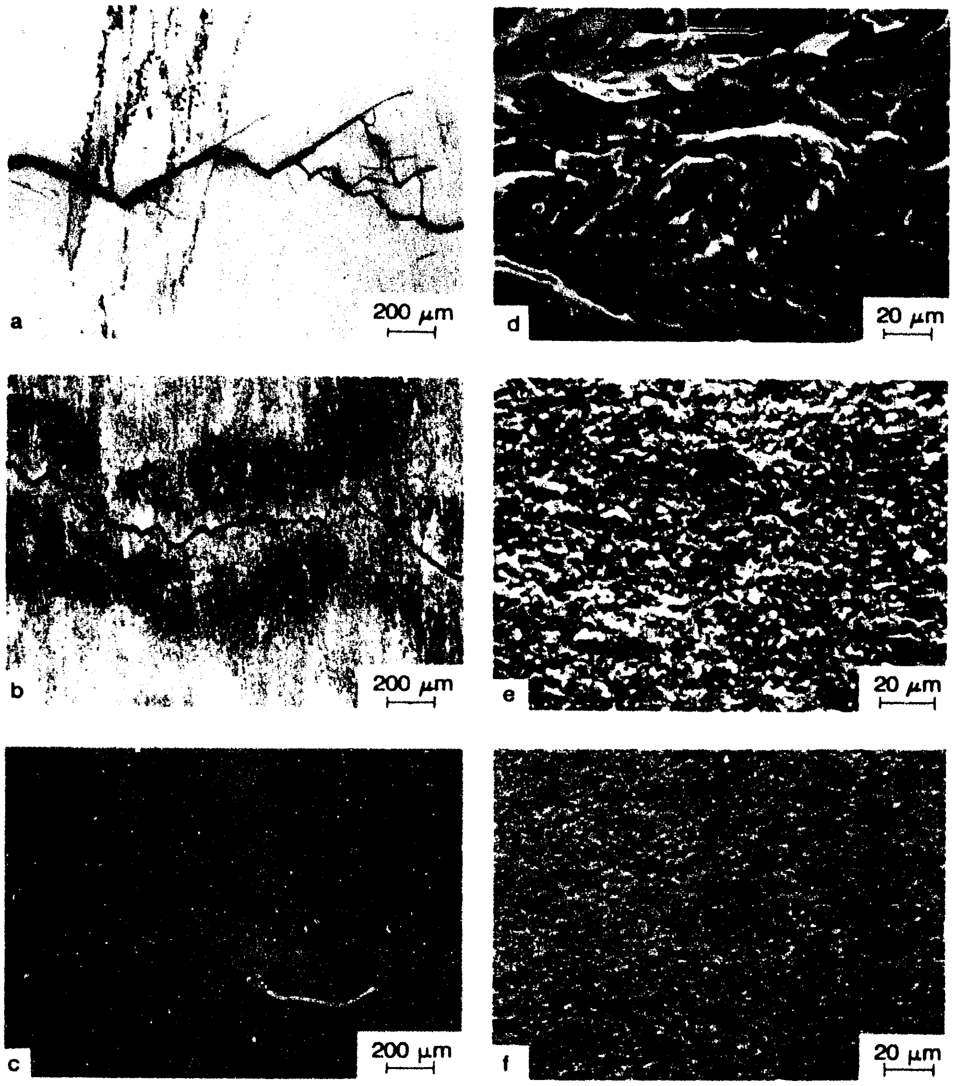

FIG. 4

(a,b,c) Optical micrographs of fatigue-crack paths and (d,e,f) scanning electron micrographs of corresponding fracture surfaces, in (a,d) I/M 2090-T81, (b,e) RSP 644-B and (c,f) MA 905-XL Al-Li alloys. Micrographs obtained for ΔK levels between 4-6 MPa$\sqrt{m}$ (L-T orientation, R = 0.1); arrow indicates general direction of crack propagation. (XBB 899-8156)

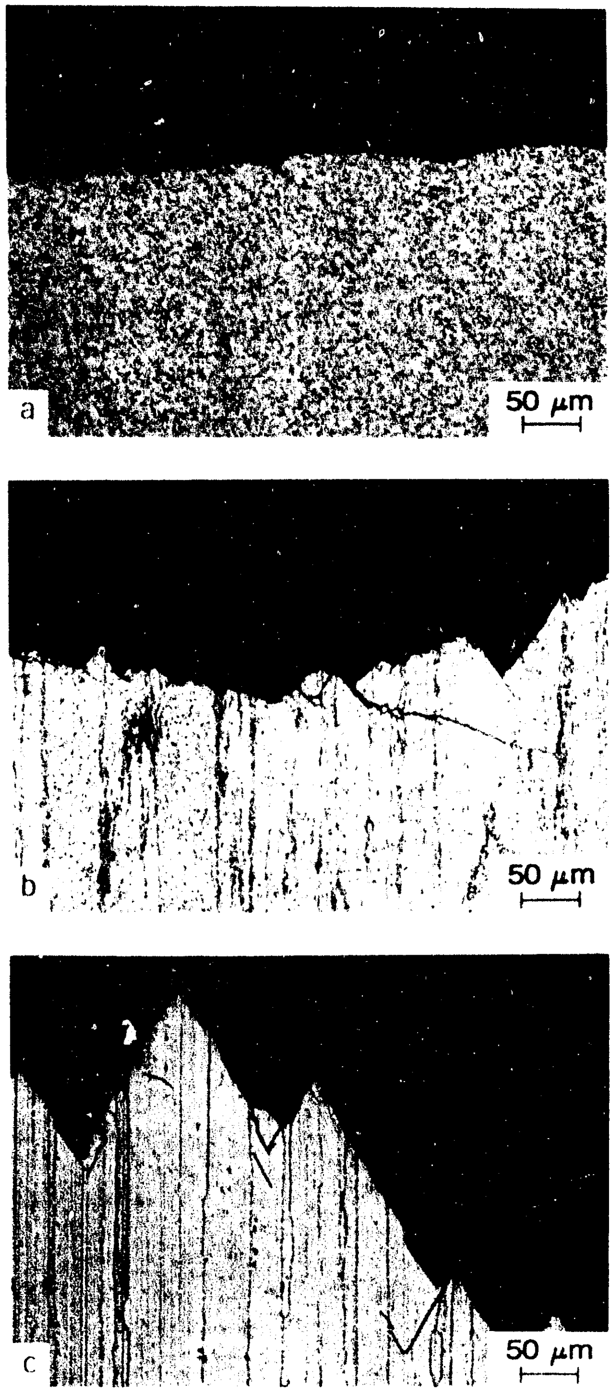

FIG. 5

Through-thickness crack-path tortuosity observed during fatigue-crack growth in (a) MA AL 905-XL, (b) RSP 644-B and (c) I/M 2090-T81 alloys. Micrographs obtained by sectioning perpendicular to the crack-growth direction and crack-growth plane. (XBB 899-8151)

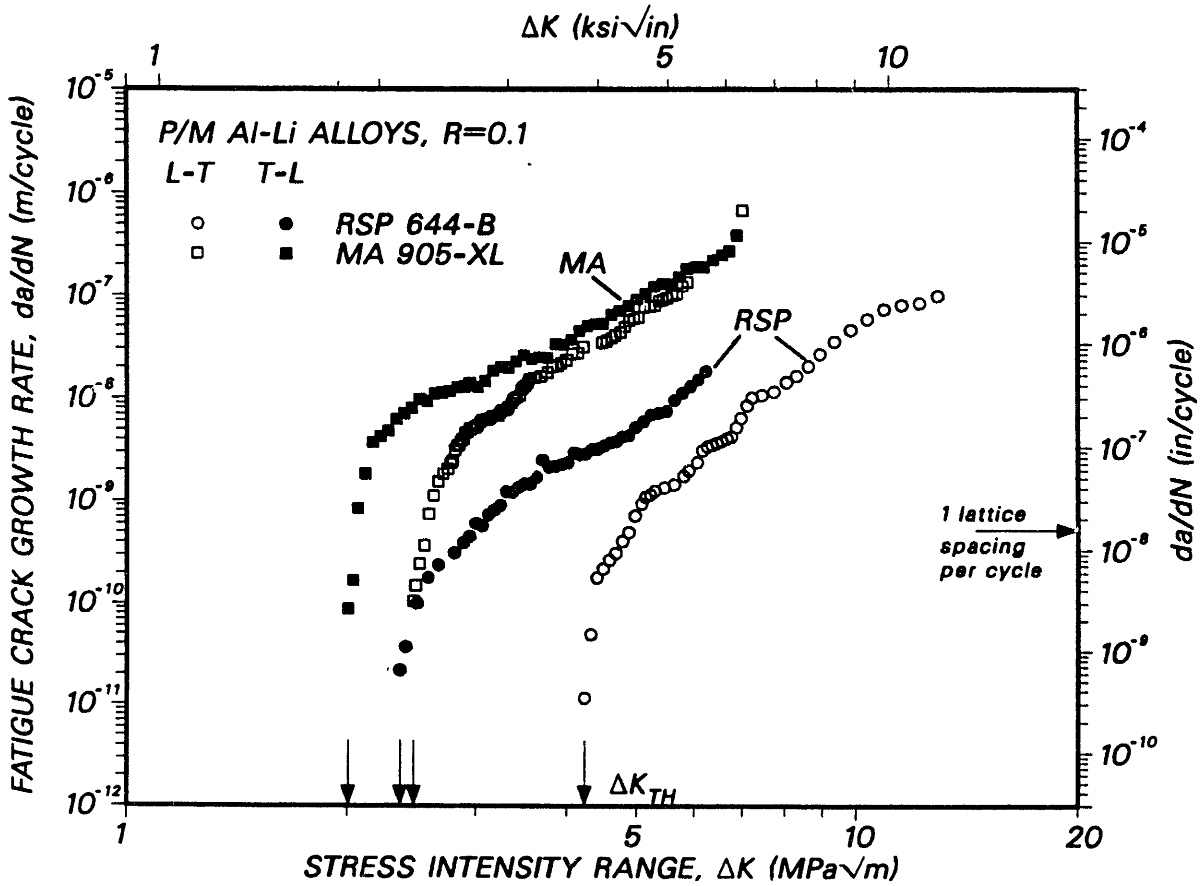

XBL 901-252

FIG. 6

Influence of specimen orientation of fatigue-crack growth rates in P/M AL 905-XL and 644-B Al-Li extrusions, at R = 0.1. Note that behavior in the L-T orientation, which is loaded along the extrusion direction (E/D), is superior compared to T-L, where loading is normal to the E/D.

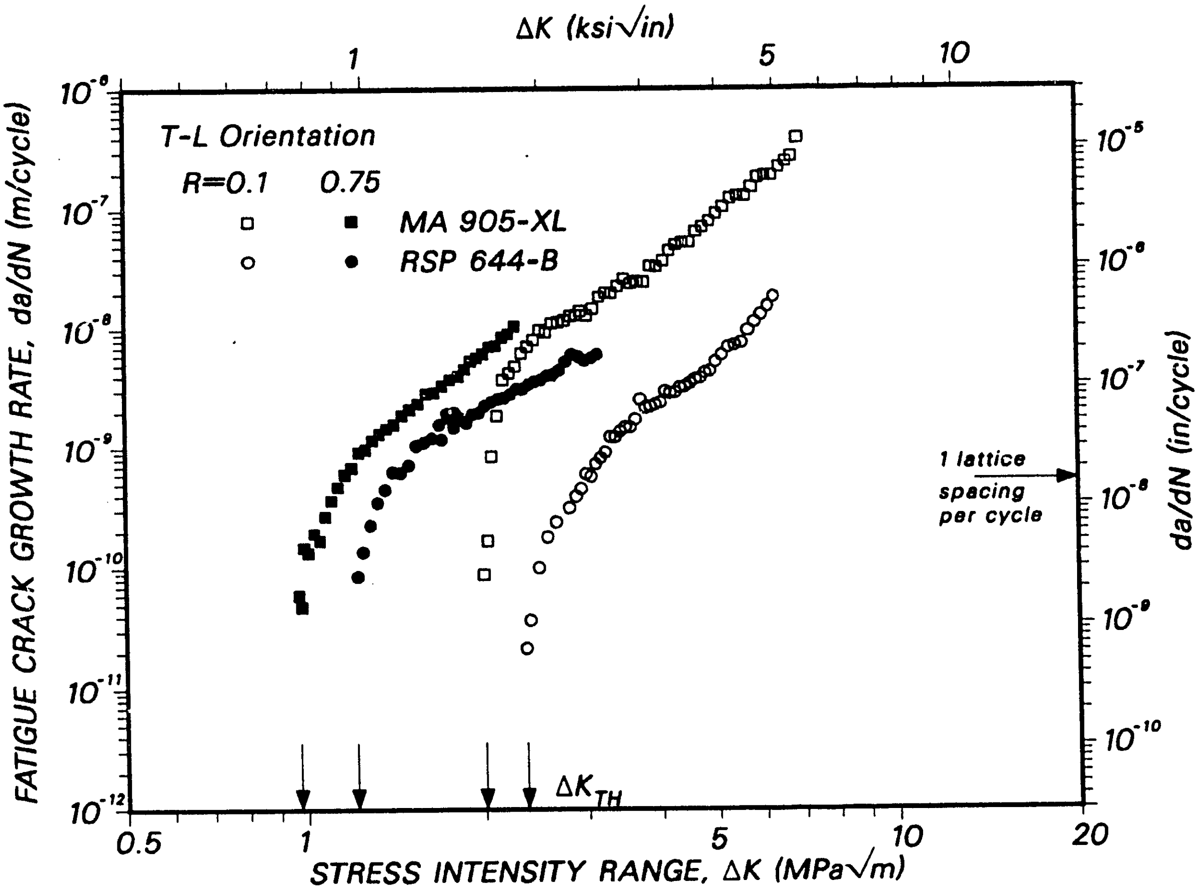

XBL 901-253

FIG. 7

Influence of load ratio ($R = K_{min}/K_{max}$) on fatigue-crack growth rates in P/M AL 905-XL and 644-B P/M Al-Li alloys. Note that behavior in MA 905-XL is less dependent on R, which develops the lower closure levels.

END

DATE FILMED

12/02/91